OPEN ACCESS
JOURNAL OF ADVANCED DIELECTRICS
Vol. 13, No. 3 (2023) 2243002 (5 pages)

DOI: 10.1142/S2010135X22430020

Ferroelastic and 90° ferroelectric domains in Bi_2WO_6 single crystals*

Xianghan Xu, Fei-Ting Huang and Sang-Wook Cheong†
Department of Physics and Astronomy, Rutgers University, Piscataway, NJ 08854, USA
†*sangc@physics.rutgers.edu*

Received 13 October 2022; Revised 12 December 2022; Accepted 18 December 2022; Published 22 February 2023

High-quality single crystals of Bi_2WO_6 are grown using a flux method. With different flux growth recipes, we aim to control the crystallization temperature to be lower and higher than the ferroelectric transition temperature, resulting in mono-domain and multi-domain Bi_2WO_6 crystals, respectively. Abundant ferroelastic orthorhombic twin domains are observed in the multi-domain crystals under an optical microscope. PFM studies unveil the 90° polarization change across those ferroelastic domain walls, as well as the absence of 180° ferroelectric domains in the as-grown multi-domain crystals, indicating a high energy cost of 180° ferroelectric domains. Moreover, a 45° tilt of the 90° ferroelectric domain walls is discovered, and this tilt creates a new type of charged 90° ferroelectric walls, which have not been observed in other bulk ferroelectrics.

Keywords: Flux growth; ferroelectric; Aurivillius phase; twin domains; PFM.

1. Introduction

Ferroelectricity was first discovered in 1920.[1] The intrinsic binary states and the electrically switchable nature enable wide applications of ferroelectric materials in electronics. More than 100 years later, the investigation of unconventional ferroelectrics in either bulk and thin film forms,[2,3] new ferroelectric mechanisms,[4] and the coupling between ferroelectricity with other physical properties[5,6] is still attracting huge research interests for achieving next-generation quantum devices. In the famous perovskite-based ferroelectrics family, the lattice instability below Curie temperature drives the lattice to a lower symmetry state, and the ferroelectricity is directly coupled with one polar lattice mode. Examples include $BaTiO_3$[7] and $Pb(Zr,Ti)O_3$.[8] In layered perovskites, such as Ruddlesden–Popper (R–P) phase and Dion–Jacobson (D–J) phase, researchers discovered that a trilinear combination of nonpolar lattice modes could also create noncentrosymmetric lattices and ferroelectricity, i.e., a hybrid improper ferroelectricity. Examples include $(Ca,Sr)_3Ti_2O_7$,[9] $Sr_3Sn_2O_7$,[10] $Ca_3Ru_2O_7$,[11] and $CsBiNb_2O_7$.[12] Exotic phenomena such as negative thermal expansion,[13] abundant (charged) domain structures,[9] and elastic-coupled ferroelectricity[14] are experimentally demonstrated.

Bi_2WO_6 belongs to an Aurivillius layered perovskite,[15,16] which is closely related to the R–P phase and D–J phase mentioned above. The ferroelectricity with a relatively large remnant polarization value ~20 $\mu C/cm^2$ has been reported in Bi_2WO_6 bulk single crystals.[17] Complex polar domain configuration as well as ferroelastic switching have been observed in Bi_2WO_6 thin films.[18] Photocatalysis activities at charged polar domain walls are also reported.[19] All those findings suggest that Bi_2WO_6 is a promising candidate for next-generation multi-functional ferroelectrics. However, despite previous thin film work, the ferroelectric domain configuration and domain engineering of Bi_2WO_6 bulk single crystal have not been studied yet.

Here, we report the growth of Bi_2WO_6 single crystal via a flux method. The strategy to tune the crystallization temperature by initial mixture recipe successfully obtains two kinds of samples, mono-domain crystals and multi-domain crystals. The optical microscope and piezoresponse force microscopy (PFM) studies reveal abundant 90° ferroelectric domains and the absence of 180° polar domains. A 45° tilt of 90° ferroelectric domain wall is observed, creating an anomalous type of charged 90° ferroelectric wall which has not been observed in other layered perovskite bulk ferroelectrics. Our finding provides insight into the intrinsic domain configuration and domain manipulation in bulk Bi_2WO_6-based materials.

2. Experimental Methods

Bi_2WO_6 single crystals were grown using a flux method with two different recipes discussed in the main text. X-ray diffraction (XRD) was carried out on the ground powder of Bi_2WO_6 crystals at 300 K using the X'Pert3 Powder diffractometer from Malvern Panalytical. The pattern was fitted using a whole pattern approach based on the Le Bail method as implemented in the GSAS software. Optical microscope images were taken in a polarized optical microscope (Zeiss Axio Imager M1m) at room temperature in the transmission

*This paper was originally submitted to the Special Issue on Ferroic Domains and Related Functionalities organized by Xueyun Wang, Houbing Huang, Jing Wang and Zhonghui Shen.

†Corresponding author.

geometry. PFM was performed on a polished *ab*-plane using a Veeco MultiMode scanning probe microscope with a Nanoscope IIIa controller. The *P–E* loops were measured by the positive up negative down (PUND) method provided in the Ferroelectric Material Test System (Radiant Technologies).

3. Results and Discussion

Bi_2WO_6 crystallizes in a noncentrosymmetric $P2_1ab$ space group at room temperature. As shown in Fig. 1(a), the fitting of XRD pattern taken on ground crystals gives lattice parameters $a = 5.437(4)$ Å, $b = 5.458(0)$ Å, and $c = 16.430(5)$ Å, which are in good agreement with the published results.[20] This crystal structure breaks all mirror symmetries perpendicular to *a*-axis, creating a polarization along *a*-axis. Polarization versus electric field (*P–E*) measurement is performed on a polished [110] plate of an as-grown Bi_2WO_6 crystal to characterize ferroelectricity. A PUND method is used to extract the remnant polarization component. As shown in Fig. 1(c), the clear hysteresis behaviors in obtained *P–E* loops demonstrate polarization switchable by electric fields; thus, the Bi_2WO_6 crystal studied here is a ferroelectric material with remnant polarization of around 20 $\mu C/cm^2$ and coercive field of around 106 kV/cm (converted to the polarization direction), which are close to reported values in literatures.[17]

In ferroelectric materials, 180° switching path essentially exists. Besides, allowed by certain lattice symmetry, non-180° polar domains may also exist. Famous examples include the 71° and 109° ferroelectric domains in $BiFeO_3$, and 90° orthorhombic twin-type ferroelectric domains in layered perovskite-based ferroelectrics. Bi_2WO_6 has an Aurivillius phase orthorhombic crystal structure which also belongs to the layered perovskite family, so 90° domains have a good chance to show up. Typically, ferroelectric domain density strongly depends on the thermal history when cooling across the T_c.[21] Inspired by a previous study that Bi_2WO_6 single crystals can crystallize within a wide concentration range in a Na_2WO_4 flux,[17] tuning the Bi_2WO_6–Na_2WO_4 molar ratio seems an effective way to manipulate the domain density in as-grown Bi_2WO_6 single crystals.

Figure 2(a) describes two recipes used to grow two batches of crystals. Sample #1 was grown by cooling the molten mixture of Bi_2WO_6:Na_2WO_4 = 1:3 from 920°C to 620°C, and sample #2 was grown by cooling the molten mixture of Bi_2WO_6:Na_2WO_4 = 1:1 from 980°C to 920°C. The cooling rate was 3°C/h in both growths. After the slow cooling, the furnace was turned off to naturally cool down to room temperature. In Fig. 2(a), the purple solid line displays the solidification temperature for mixtures with certain Bi_2WO_6 concentration in the mixture, and the horizontal dashed line

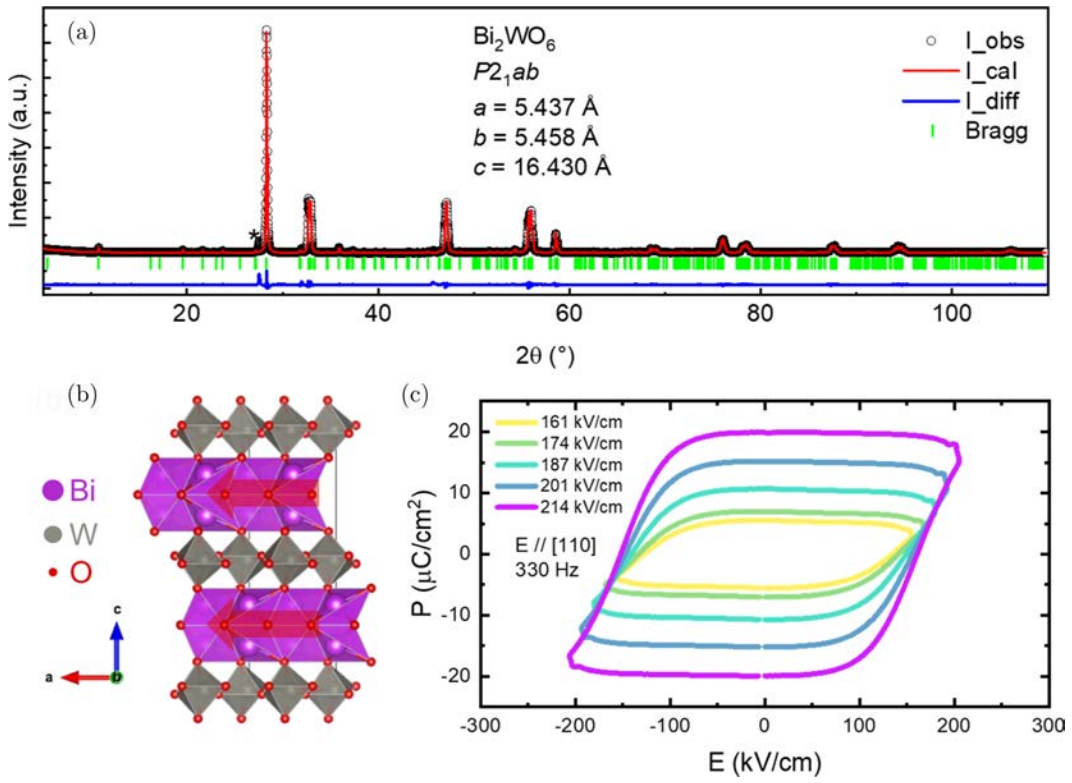

Fig. 1. (Color online) (a) The Le Bail fitting the XRD pattern of ground as-grown Bi_2WO_6 crystals. The asterisk marks a peak possibly from residual flux attached on the crystal. (b) Crystal structure of Bi_2WO_6. The polarization is parallel to *a*-axis denoted by the red arrows. (c) The polarization versus electric field loops measured with electric field parallel to [110] direction of a Bi_2WO_6 crystal. The frequency of electric field is 330 Hz.

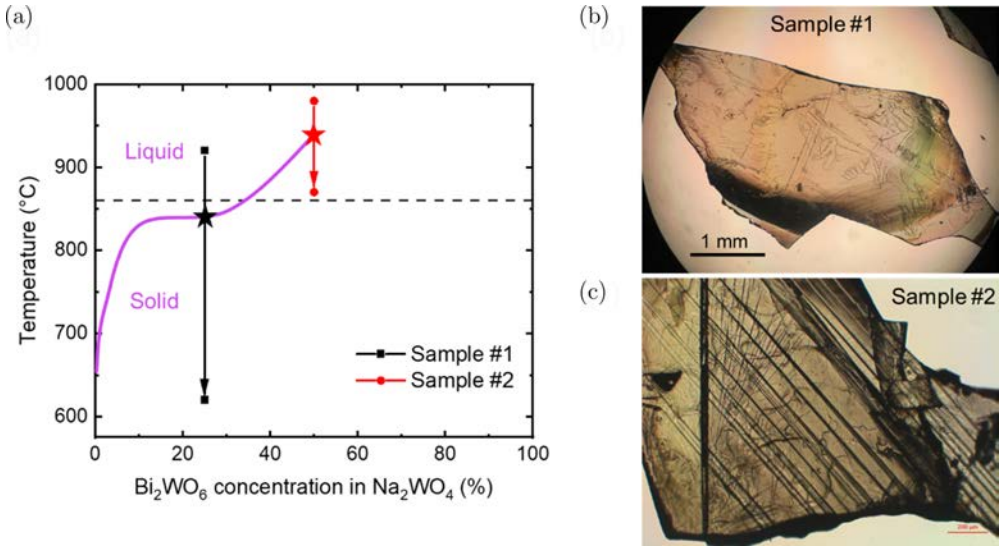

Fig. 2. (Color online) (a) The growth recipe of samples #1 and #2. The purple line denotes the boundary of liquid and solid states of the Bi_2WO_6–Na_2WO_4 mixture, which is extracted from Ref. 17. (b) and (c) The optical microscope images of samples #1 and #2.

represents the ferroelectric Curie temperature (T_c) ~860°C. Based on this qualitative phase diagram, the crystallization happens at a temperature above the T_c for sample #1, but below the T_c for sample #2, as marked by the black and red stars, respectively. We will next show those difference growth temperature ranges give rise to distinct structural domain configurations.

Optical microscope images are performed on samples #1 and #2 using cross-polarizers geometry. As shown in Fig. 2(b), sample #1 which crystallized below the ferroelectric T_c does not show any observable domains under polarized transmission light optical microscope, while there are clear stripy domains with typical width 10–100 μm observed in sample #2 which crystallized above the ferroelectric T_c. This type of stripy domain has been commonly observed in orthorhombic crystals, i.e., 90° ferroelectric domains. Unlike the 90° ferroelectric domains which exhibit birefringence in the orthorhombic symmetry, the 180° ferroelectric domains cannot be detected by optical microscope method,[22] but may also exist in ferroelectric Bi_2WO_6. To confirm the 90° polarization change across the observed domain walls and to map out the completed domain configuration, PFM measurements are performed on a piece of multi-domain sample #2. As shown in Fig. 3(a), the topology of the polished surface of a selected area does not show any contrast except polish marks, but the in-plane piezoelectric response intensity image in Fig. 3(b) clearly exhibits the stripy domains consistent with the observation in optical microscope images. Figures 3(d) and 3(e) display the in-plane PFM results after a 45° clockwise sample rotation. In the domain wall perpendicular to cantilever case (Fig. 3(b)), the PFM signals of two domains show significant differences, ruling out the head-to-head or tail-to-tail case, since in those cases the two domains would have the same in-plane polarization component perpendicular to the cantilever. The purple arrows display the polarization configuration that is consistent with the crystallographic orientation and the PFM results. It confirms the 90° polarization change across those domain walls seen in optical microscope. Unlike many hybrid improper ferroelectric layered perovskites, no 180° ferroelectric domains are observed in the PFM data. In other words, each orthorhombic twin domain is a single ferroelectric domain in as-grown Bi_2WO_6. Generally, the multi-domain or mono-domain state of ferroelectric crystals is a result of competing depolarization field (favor multi-domain) and lattice mismatching energy cost (favor mono-domain). A possible explanation for observed single domain in the sample crystallized below T_c is that the crystallization nucleation center is already polar, so lattices grown on it tend to possess the same polarizations to minimize lattice mismatching energy, and at the crystal growth high temperatures, the depolarization field may be screened by conduction.

As shown in Fig. 2(c), the 90° ferroelectric domains uniformly exist in sample #2. However, in some specific regions, an anomalous type of ferroelectric domain is observed. Figure 4(a) shows the polished surface of the selected scanning area, and the PFM image of that area (Fig. 4(b)) clearly shows a 45° tilt of the 90° ferroelectric domain wall (from black dashed line to the red dashed line), which creates a discontinuity of polarization component perpendicular to the domain wall, i.e., a charged domain wall.

Overall, there are two main differences between the observed domain configuration of Bi_2WO_6 crystal and previously studied R–P phase hybrid improper ferroelectrics such as $(Ca,Sr)_3Ti_2O_7$ and $Sr_3Sn_2O_7$. First, abundant charged 180° walls were reported in $(Ca,Sr)_3Ti_2O_7$ and $Sr_3Sn_2O_7$ crystals, but here we do not find any 180° walls in Bi_2WO_6 crystals. A possible reason is that Bi_2WO_6 holds much larger remnant polarization magnitude, hence the system lowers its

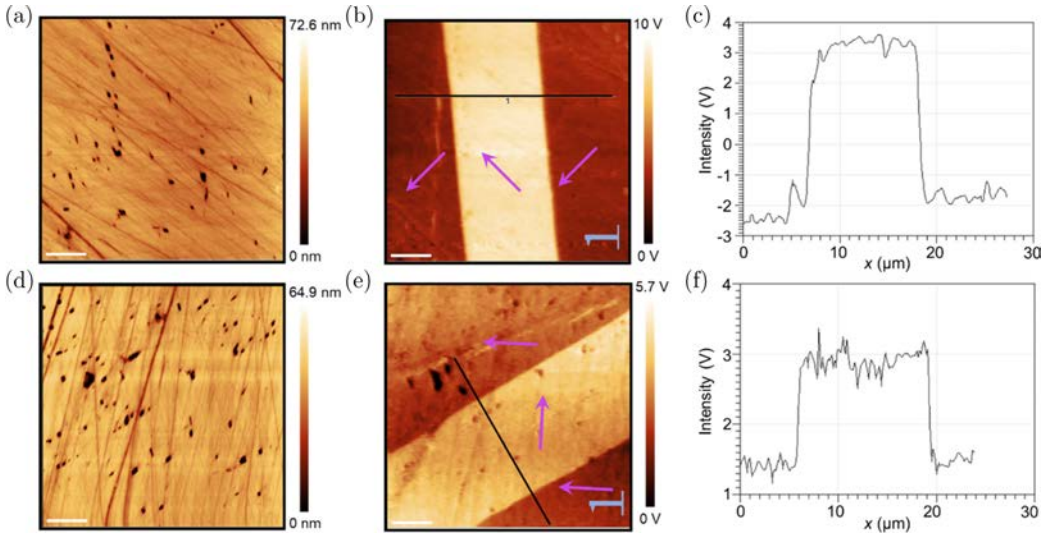

Fig. 3. (a) The topology of a selected scanning area of sample #2. The white scale bars are 5 μm. (b) The in-plane PFM intensity of the same area as in (a). (c) The line profile of the PFM signal marked by the solid line in (b) crossing three domains. (d) and (e) The topology and PFM results after rotating the sample by clockwise 45°. (f) The line profile of the PFM signal marked by the solid line in (e) crossing three domains.

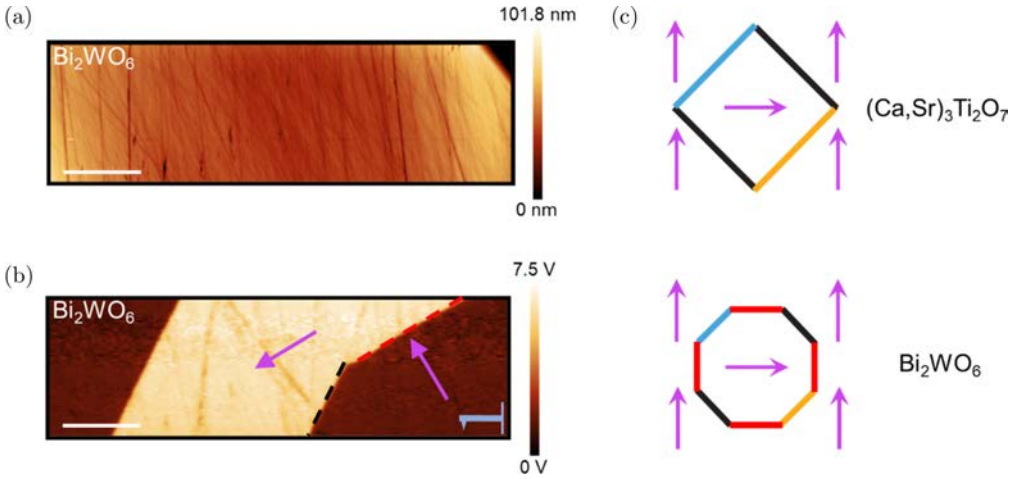

Fig. 4. (Color online) (a) The topology of a selected scanning area. The white scale bars are 20 μm. (b) The PFM response of the same area as in (a). The black and red dashed lines represent the regular 90° ferroelectric domain wall and anomalous charged wall. (c) The schematic illustration comparing the 90° ferroelectric domain configuration observed in Bi_2WO_6 with the reported $(Ca,Sr)_3Ti_2O_7$.

electrostatic energy by avoiding 180° walls. Second, four types of 90° ferroelectric domain wall geometry were found in $(Ca,Sr)_3Ti_2O_7$ and $Sr_3Sn_2O_7$ crystals as demonstrated in Fig. 4(c) upper panel. However, the existence of 45° tilt of 90° ferroelectric walls in Bi_2WO_6 crystals indicates more complicated ferroelectric wall types as shown in Fig. 4(c) lower panel. In the Bi_2WO_6 case, eight types of 90° ferroelectric walls exist and four of them are supposed to be charged.

4. Conclusion

Bi_2WO_6 single crystals are synthesized via a flux method. Tuning the recipe leads to mono-domain crystals and multi-domain crystals depending on the crystallization temperature lower or higher than the ferroelectric T_c. Using optical microscope and PFM techniques, abundant ferroelastic orthorhombic twin domains are observed in the multi-domain crystals, which are also 90° ferroelectric domains. The 45° tilt of the 90° ferroelectric walls produces a new type of 90° ferroelectric walls that are possibly charged. No hints of 180° walls are observed. In the future, deeper investigations on the observed 45° tilt wall utilizing advanced experimental techniques such as electron diffraction are desired to unveil if it is coherent in terms of crystallography. Our work reveals the domain configuration and paves the road for domain engineering in Bi_2WO_6 bulk materials. Our work also suggests that the local conduction and photocatalysis behavior at the possibly charged domain walls and the domain switching

kinetics in bulk Bi_2WO_6 are promising topics to be studied in future.

Acknowledgments

This work was supported by the Center for Quantum Materials Synthesis (cQMS), funded by the Gordon and Betty Moore Foundation's EPiQS initiative through grant GBMF10104, and by Rutgers University.

References

[1]J. Valasek, Piezo-electric and allied phenomena in Rochelle salt, *Phys. Rev.* **17**, 475 (1921).
[2]N. Setter and E. Colla, *Ferroelectric Ceramics*: *Tutorial Reviews, Theory, Processing, and Applications* (Springer, 1993).
[3]L. W. Martin and A. M. Rappe, Thin-film ferroelectric materials and their applications, *Nat. Rev. Mater.* **2**, 16087 (2016).
[4]N. A. Benedek and C. J. Fennie, Hybrid improper ferroelectricity: A mechanism for controllable polarization-magnetization coupling, *Phys. Rev. Lett.* **106**, 107204 (2011).
[5]S.-W. Cheong and M. Mostovoy, Multiferroics: A magnetic twist for ferroelectricity, *Nat. Mater.* **6**, 13 (2007).
[6]N. A. Spaldin and R. Ramesh, Advances in magnetoelectric multiferroics, *Nat. Mater.* **18**, 203 (2019).
[7]G. Shirane, F. Jona and R. Pepinsky, Some aspects of ferroelectricity, *Proc. IRE* **43**, 1738 (1955).
[8]T. M. Kamel and G. de With, Poling of hard ferroelectric PZT ceramics, *J. Eur. Ceram. Soc.* **28**, 1827 (2008).
[9]Y. S. Oh, X. Luo, F.-T. Huang, Y. Wang and S.-W. Cheong, Experimental demonstration of hybrid improper ferroelectricity and the presence of abundant charged walls in $(Ca,Sr)_3Ti_2O_7$ crystals, *Nat. Mater.* **14**, 407 (2015).
[10]Y. Wang, F.-T. Huang, X. Luo, B. Gao and S.-W. Cheong, The first room-temperature ferroelectric Sn insulator and its polarization switching kinetics, *Adv. Mater.* **29**, 1601288 (2017).
[11]S. Lei, M. Gu, D. Puggioni, G. Stone, J. Peng, J. Ge, Y. Wang, B. Wang, Y. Yuan, K. Wang, Z. Mao, J. M. Rondinelli and V. Gopalan, Observation of quasi-two-dimensional polar domains and ferroelastic switching in a metal, $Ca_3Ru_2O_7$, *Nano Lett.* **18**, 3088 (2018).
[12]X. Fang, R. Hu, Y. Wang, F.-T. Huang and S.-W. Cheong, Hybrid improper ferroelectricity in highly cleavable single crystals of Dion-Jacobson-compound $CsBiNb_2O_7$, *Adv. Electron. Mater.* **8**, 2100929 (2022).
[13]M. S. Senn, A. Bombardi, C. A. Murray, C. Vecchini, A. Scherillo, X. Luo and S. Cheong, Negative thermal expansion in hybrid improper ferroelectric Ruddlesden-Popper perovskites by symmetry trapping, *Phys. Rev. Lett.* **114**, 035701 (2015).
[14]X. Xu, Y. Wang, F.-T. Huang, K. Du, E. A. Nowadnick and S.-W. Cheong, Highly tunable ferroelectricity in hybrid improper ferroelectric $Sr_3Sn_2O_7$, *Adv. Funct. Mater.* **30**, 2003623 (2020).
[15]A. Peláiz-Barranco and Y. González-Abreu, Ferroelectric ceramic materials of the Aurivillius family, *J. Adv. Dielectr.* **3**, 1330003 (2013).
[16]A. Moure, Review and perspectives of Aurivillius structures as a lead-free piezoelectric system, *Appl. Sci.* **8**, 62 (2018).
[17]K. Muramatsu, A. Watanabe and M. Goto, Flux growth of Bi_2WO_6 single crystal below the transformation temperature, *J. Cryst. Growth* **44**, 50 (1978).
[18]C. Wang, X. Ke, J. Wang, R. Liang, Z. Luo, Y. Tian, D. Yi, Q. Zhang, J. Wang, X.-F. Han, G. Van Tendeloo, L.-Q. Chen, C.-W. Nan, R. Ramesh and J. Zhang, Ferroelastic switching in a layered-perovskite thin film, *Nat. Commun.* **7**, 10636 (2016).
[19]R. Ullah, M. Pei, J. Wu, Y. Tian, Z. Gu, Q. Zhang, C. Song, Y. Yang, M. Ahmad, J. Zeb, F. Qayyum, Y. Liu, X. An, L. Gu, X. Wang and J. Zhang, Bifunctional photoelectrode driven by charged domain walls in ferroelectric Bi_2WO_6, *ACS Appl. Energy Mater.* **3**, 4149 (2020).
[20]H. Okudera, Y. Sakai, K. Yamagata and H. Takeda, Structure of russellite (Bi_2WO_6): Origin of ferroelectricity and the effect of the stereoactive lone electron pair on the structure, *Acta Crystallogr. B* **74**, 295 (2018).
[21]S.-Z. Lin, X. Wang, Y. Kamiya, G.-W. Chern, F. Fan, D. Fan, B. Casas, Y. Liu, V. Kiryukhin, W. H. Zurek, C. D. Batista and S.-W. Cheong, Topological defects as relics of emergent continuous symmetry and Higgs condensation of disorder in ferroelectrics, *Nat. Phys.* **10**, 970 (2014).
[22]G. Tang, L. Wen, H. Xing, W. Liu, J. Peng, Y. Wang, Y. Li, B. Lv, Y. Yang and C. Yao, Structural domain imaging and direct determination of crystallographic orientation in noncentrosymmetric $Ca_3Ru_2O_7$ using polarized light reflectance, *Chin. Phys. Lett.* **37**, 106102 (2020).